Hindawi
Journal of Energy
Volume 2022, Article ID 2944552, 10 pages
https://doi.org/10.1155/2022/2944552

Research Article

Syngas Production from Agriculture Residues: Sudan

Ali A. Rabah

Department of Chemical Engineering, University of Khartoum, P.O. Box 321, Khartoum, Sudan

Correspondence should be addressed to Ali A. Rabah; rabahaa1967@gmail.com

Received 18 December 2021; Revised 1 February 2022; Accepted 2 February 2022; Published 21 February 2022

Academic Editor: Ciro Aprea

The study is aimed at evaluating the availability of agriculture residues for syngas production, a case study for Sudan. 10 types of biomass are investigated: sugarcane (bagasse), cotton stalks, sesame straw, groundnut shells, maize straw, sorghum straw, millet straw, sunflower husks, wheat straw, and banana leaves. The available biomass is about 11 Mt/year (3.68 Mtoe). Aspen plus software is applied to simulate the gasification process. The study covered a wide range of operating conditions of steam to biomass ratio ($0 < SB < 2$) and equivalent ratio ($0 > ER > 0.5$). For all types of syngas characteristics, H_2 is 0.32-0.42 (mole fraction), CO is 0.13 to 0.16 (mole fraction), LHV is 5.0 to 8.0 MJ/kg, and the yield is ≥1.5. Wheat, groundnut, and sunflower have the best characteristics, while millet and bagasse yield the poorest characteristics. In addition, all types of syngas have $H_2/CO > 2$ except Millet. These characteristics make all types of syngas except millet suitable for both energy and industry applications. The potential syngas production is 14.17 Mt/year.

1. Introduction

In Sudan, agricultural residues are poorly managed. They are left in the field to decompose or burn as a part of land preparation. Burning results in significant CO_2 emissions. Table 1 shows Sudan's available biomass from agricultural residue, excluding grass and forestry. The available biomass for energy also excludes that goes as animal feed, construction, and other industries. The available biomass for energy is about 11 Mt/year, with an energy content of 154 PJ/year (154×10^{15} J), equivalent to 3.68 Mtoe ($1\,TJ = 2.388 \times 10^{-5}$ Mtoe) [1–4]. The potential electric generation from biomass is about 1 GW. Sudan biomass potential could increase four times the current amount. Sudan cultivable land is estimated at 74 million hectares, only 25% of which is currently used [5].

Due to the growing world population, the food, energy, and environmental conservation demands are high. One of the mitigation measures to sustain energy production in the event of fossil oil depletion is to cut fossil fuel consumption. Renewable energy, in particular, biomass is a promising candidate that can ensure sustainable energy production and environmental conservation [8]. Many studies on the performance of biomass in cogeneration (combined heat and power (CHP)) have been reported in the literature [8–11].

$$(AAR) = (AAP)(RPR)(A). \quad (1)$$

The previous literature on the biomass understudy indicated that all biomass listed in Table 1 have been studied except sesame [11–14]. The studies covered chemical and physical properties (the ultimate and approximate analysis and calorific values), the performance in CHP, and syngas production. However, search on sesame stalks meets no hits on syngas and CHP; only hits on chemical and physical properties are met.

The chemical energy in biomass is converted into energy via thermochemical processes. Syngas production is an example of biomass gasification. Syngas is a gas mixture of H_2, CO, CO_2, and CH_4. It is utilized in power generation, fuel synthesis using the Fischer-Tropsch process, and ammonia production. Gasification advantages over direct combustion are low NO_x emissions [15]; direct combustion occurs at a high temperature > 1300°C, which is favorable to NO_x formation. The net CO_2 emission of biomass in gasification is zero [16, 17]. It can be concluded

Table 1: Available biomass per year (Sudan) [2–4, 6].

No	Biomass	Residue	AAP[1]	RPR[2]	A3	AAR[4]	LHV	Energy	Mtoe
			Ton		%	Ton	MJ/kg	TJ	
1	Sugarcane	Bagasse	5525059	0.30	40.00	663007.08	18.00	11934.13	0.2850
2	Wheat	Straw	516000	0.80	15.00	61920.00	18.20	1126.94	0.0269
3	Cotton	Stalks	4572	2.70	60.00	7406.64	18.61	137.84	0.0033
4	Sesame	Straw	525000	0.50	56.00	147000.00	12.40	1822.80	0.0435
5	Groundnut	Shells	1826000	0.48	40.00	350592.00	15.66	5490.27	0.1311
6	Sorghum	Straw	6466000	1.25	60.00	4849500.00	12.38	60036.81	1.4337
7	Millet	Straw	1449000	1.75	60.00	1521450.00	12.39	18850.77	0.4502
8	Bananas	Leaves	910110	0.70	60.00	382246.20	15.90	6077.71	0.1451
9	Sunflower	Husk	108000	0.60	60.00	38880.00	14.20	552.10	0.0132
10	Maize	Straw	25000	1.00	60.00	15000.00	18.50	277.50	0.0066
11	Tobacco	Stalks	182888	0.70	60.00	76812.96	17.30	1328.86	0.0317
12	Mango	Seed	7885940	0.50	80.00	3154376.00	15.00	47315.64	1.1299
	Total					11268190.88		154951.37	3.68

[1]AAP: the available Amount of Agricultural Product in ton; [2]RPR: Residue to Product Ratio; [3]A: the Availability of residues; [4]AAR: the available Amount of Agricultural Residues in ton is estimated using the model of Karaca et al. [7] given in equation (1).

that biomass is a sustainable energy source and a solution to the CO_2 emissions.

The key gasification steps are drying, pyrolysis, combustion (oxidation reactions), gasification (reduction reactions), and gas cleaning. The first four processes occur inside the reactor, while gas cleaning occurs outside. Drying or moisture removal occurs at 100°C–200°C. Drying heat demand could be supplied from recovered heat. The dried biomass undergoes thermal decomposition through the pyrolysis process at a temperature between 350°C and 650°C according to the following chemical reaction (equation (2)) [18, 19]:

$$\underset{\text{pyrolysis gases}}{\text{Biomass} \longrightarrow \text{CO} + \text{H}_2 + \text{CO}_2 + \text{H}_2\text{O} + \text{H}_2\text{S} + N_2 + \text{CH}_4 + \text{C}_6\text{H}_6 + \text{char}}. \quad (2)$$

The char converts into syngas in the oxidation and reduction reactions as shown in Table 2. The key operating parameters are reaction temperature, steam to biomass ratio (SB), and air equivalent ratio (ER). The literature review shows the operating conditions are in the following range: the gasification temperature (500°C-1000°C), SB (0 to 2), and ER (<1) [12, 16, 17, 20, 21].

2. Materials and Methods

2.1. Biomass Characteristics. Table 3 shows proximate and ultimate analyses of different biomass. The chemical compositions are in the following range: 30–53% C, 38–55% O_2, 3.0–6.3% H_2, <2% N_2, <1% S, and 2-11% ash. Except bagasse, the moisture content is in the range of 3-11.5% while for bagasse it is about 50%. C/N of all biomass is greater than 30. The data are reproduced the way presented in the literature although the proximate composition (FC, VM, and ash) does not add to 100%, similarly the ultimate analysis.

2.2. Aspen plus Simulation. Due to its capability to process solids, Advanced System for Process Engineering (Aspen) Plus software is a widely used package in the modeling and simulation of biomass gasification process [28]. The process flow diagram (PFD) for biomass gasification is almost standard. It consists of four blocks: drying, pyrolysis (decomposition), char gasification, and gas cleaning. RStoic, RYield, and RGibbs reactors are used for drying, pyrolysis, and char gasification, respectively. In gas cleaning, a cyclone and a flash separator facilitate ash and water removal, respectively [20].

The modeling and simulation of the biomass gasification process are performed with Aspen Plus v10 software. Biomass is defined as a nonconventional component through its ultimate and proximate analysis. Sulfate and carbon are defined as solids. The fluid package of Peng–Robinson (PR-ROB) equation of state is selected to evaluate all physical properties of the conventional components. HCOALGEN and DCOALGEN models are selected for the evaluation of the enthalpy and density of both biomass and ash.

Figure 1 shows the biomass gasification PFD. The wet biomass is fed into the "RStoic" reactor block (R-101), where moisture is liberated. The RStoic outlet stream (stream 2) goes into the separator (V-101), which separates the stream into moisture (stream 4) and dry biomass (stream 4). The dry biomass passes to the "RYield" reactor (R-102) for pyrolysis. The RYield reactor block calculates the yield distribution of the products without the need to specify reaction stoichiometry and reaction kinetics [31]. The "RYield" reactor converts biomass into conventional components (O_2, H_2, N_2, H_2O, S, tar, and char). The pyrolysis products (stream 5) are fed to the RGibbs reactor (R-103). The option of

Table 2: Biomass gasification chemical reactions.

Phase	Reaction name	Biomass gasification	ΔH_r [kJ/mole]
Oxidation	Combustion	$C + O_2 = CO_2$	-394
	Partial combustion	$C + 0.5O_2 = CO$	-111
	Combustion	$H_2 + 0.5O_2 = H_2O$	-242
Reduction	C-water reaction	$C + H_2O \leftrightarrow CO = H_2$	131
	Boudouard reaction	$C \leftrightarrow CO_2 \leftrightarrow 2CO$	172
	C-Methanation	$C + H_2 \leftrightarrow CH_4$	-75
	Water gas shift	$CO + H_2O \leftrightarrow CO_2 + H_2$	41
	Steam reforming	$CH_4 + H_2O \leftrightarrow CO + 3H_2$	206
	Steam reforming	$CH_4 + 2H_2O \leftrightarrow CO_2 + 4H_2$	206

Table 3: Biomass proximate and ultimate analysis.

No.		Ref	FC	VM	Ash	Moisture %	C	H	O	N	S	C/N
1	Bagasse	[22]	12.23	83.01	4.76	50.00	46.95	6.06	42.44	0.13	0.08	361.15
2	Wheat	[13]	13.22	69.24	8.75	8.79	42.20	5.57	38.64	0.60	0.36	70.33
3	Cotton	[13]	16.94	71.41	3.73	7.92	44.63	5.78	43.00	0.66	0.44	67.62
4	Sesame	[13]	14.47	67.89	6.42	11.23	41.70	5.78	42.85	0.54	0.52	77.22
5	Groundnut	[23]	20.86	65.13	2.89	11.12	52.96	6.24	40.20	0.59	0.22	89.76
6	Sorghum	[24]	16.06	72.02	5.70	5.22	42.00	5.49	45.42	0.66	0.73	63.64
7	Millet	[14]	7.90	83.10	5.80	3.20	41.60	3.60	54.80	0.03	0.00	1386.67
8	Banana	[25]	7.60	83.35	9.36	6.67	33.46	6.44	49.94	0.80	0.04	41.83
9	Sunflower	[26]	24.17	75.83	10.55	10.58	49.07	6.22	43.80	0.90	0.17	54.52
10	Maize	[27]	16.03	70.31	5.25	8.42	44.20	5.80	43.50	1.30	0.01	34.00

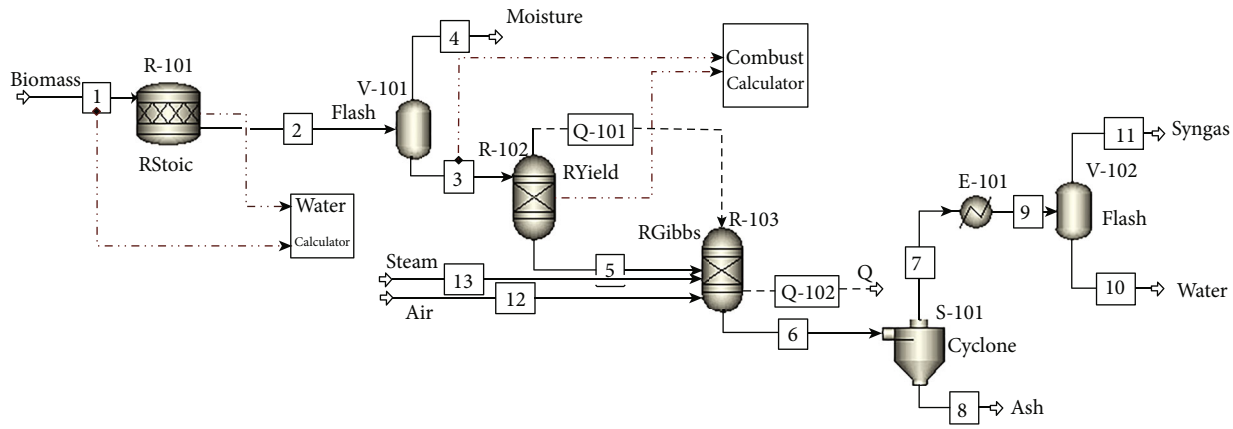

Figure 1: PFD of biomass gasification.

"Restrict chemical equilibrium-specify temperature approach or reactions" is chosen for the simulation of the RGibbs reactor. The combustion and oxidation reaction are supplied (Table 2). The RGibbs reactor outlet (stream 6) moves to the cyclone (S-101), which separates stream 6 into wet syngas (stream 7) and ash (stream 8). The wet syngas (stream 7) is cooled in the heat exchanger (E-101) and the associated water is condensed. The cold wet syngas (stream 9) goes to the flash (V-102), which separates (stream 9) into syngas (stream 11) and water (stream 10). The air (stream 12) and steam (stream 13) as gasifying agents are added to the RGibbs reactor (R-103).

3. Results and Discussion

3.1. Model Validation. The simulation model is validated using the experimental data of De Filippis et al. [29] and the simulation data of Mavukwana et al. [20]. The proximate

Table 4: Validation of simulation results (T = 850°C, SB = 1.9, ER = 0.38).

Component	This work	Ref. [29]		Ref. [20]	
	v/*v* (%)	*v*/*v* (%)	Deviation (%)	*v*/*v* (%)	Deviation (%)
H_2	45.60	40.60	10.96	49.20	-7.90
CO	11.25	17.20	-52.90	14.12	-25.52
CO_2	43.15	33.70	21.90	35.37	18.04
CH_4	00.00	8.00		00.00	

and ultimate analyses of bagasse used in the comparison are as follows:

(i) Proximate analysis (values in %): 88.7 VM, 9.3 FC, 2 ash, and 11.1 moisture

(ii) Ultimate analysis (values in %): 42.9 C, 5.9 H, 49 O, 0.2 N, 0 S, and 0 Cl_2

Table 4 summarizes the comparison results. The present work agrees with Mavukwana et al.'s [20] simulation results in the prediction of methane as both works yield no CH_4 formation. No formation of methane is a common problem experienced by many simulations works [30].

Concerning H_2, the simulation under predicts Mavukwana et al.'s [20] results by about 7% and over predicts De Filippis et al.'s [29] experimental results by about 10%. Deviations on CO and CO_2 relative to both simulation and experimental results are high. One reason is the RGibbs assumption of minimum value of the total Gibbs energy at chemical equilibrium. This assumption may not be satisfied at the experiment. Another reason is that ER and SB values may not be the optimum combination. The optimum ER and SB correspond to the point where CO and CO_2 composition crossover. More light on the optimum ER and SB conditions is shed in the subsequent sections.

3.2. Operating Conditions. The operating conditions of biomass gasification are gasification temperature, equivalent ratio (ER), and steam to biomass ratio (SB). Equivalent ratio (ER) of air is defined by

$$\mathrm{ER} = \frac{\text{Feed air [kg/h]}}{\text{Flow of stoichiometric air for complete combustion [kg/h]}}. \tag{3}$$

The stoichiometric air fuel ratio (AFR) is calculated from ultimate analysis using

$$\mathrm{AFR} = \left(\frac{|\mathrm{C}|}{12} + \frac{|\mathrm{H_2}|}{4} + \frac{|\mathrm{S}|}{32} + \frac{|\mathrm{O_2}|}{32}\right)\left(1 + \frac{79}{21}\right)\left(1 - \frac{|\mathrm{Ash}|}{100}\right)\frac{28.4}{100}. \tag{4}$$

The calculation is made on moisture and ash free basis. The steam to biomass ratio (SB) is

$$\mathrm{SB} = \frac{\text{Feed of } \mathrm{H_2O} \text{ as steam [kg/h]}}{\text{Flow of biomass [kg/h]}}. \tag{5}$$

Equivalent ratio (ER) of steam is defined by

$$\mathrm{ER_{steam}} = \frac{\text{Feed steam [kg/h]}}{\text{Flow of stoichiometric steam for complete combustion [kg/h]}}. \tag{6}$$

Stoichiometric steam to biomass ratio (SB) is

$$\mathrm{SB} = \left(\frac{|\mathrm{C}|}{12}\right)\left(1 - \frac{|\mathrm{Ash}|}{100}\right)\frac{18}{100}. \tag{7}$$

Table 5 shows ultimate and proximate analysis of data presented in Table 3 in a normalized form. The stoichiometric air to fuel ratio (AFR) and theoretical steam to biomass ratio (SB) are calculated using equations (4) and (7), respectively. Stoichiometric AFR varies between 3.18 for millet to 6.01 for groundnut. Theoretical steam to biomass ratio (SB) varies between 0.45 for banana and 0.75 for groundnut. The estimated SB does not include steam required for water gas shift and steam reforming reactions.

Figures 2(a)–4(d) show CO and CO_2 concentration against SB (0 to 2.0) for a wide range of ER (0 to 0.5). CO and CO_2 concentration profiles assume opposite trends and reach a point of crossover. The opposite trend is attributed to the competitive oxidation and reduction reactions. The point of crossover is called the carbon boundary point (CBP). It is the point where carbon is depleted or consumed. It is considered the point of optimum ER and SB combination [16, 31]. ER > 0 is needed to provide the energy demand for oxidation reactions. However, ER should not be excessive to shift the reaction towards oxidation: CO_2 production. In most studies, ER is limited to $0.13 > \mathrm{ER} > 0.5$ [20, 21]. An ER of 0.15 is considered in this work. For all biomass understudy, the corresponding SB is determined using Figures 2(a)–4(d). The CBP at ER = 0.15 is indicated by the dotted line. Figure 5 shows the SB for different biomass at the CBPs. Groundnut demands the highest SB of 1.2, and bagasse demands the lowest SB of 0.4. Groundnut has the highest carbon and hydrogen contents among the studied biomass. The steam demand for C-water reaction and Water-gas shift reaction is higher than that required by the other biomasses. The low SB demand for bagasse is attributed to the high moisture content. The moisture is controlled at 10% in the simulation process for those biomasses with higher moisture. The other biomasses have a moisture content of less than 10%.

Another feature that can be seen in Figures 2(a)–4(d) is the point of crossover of all CO_2 curves at one point. The

Table 5: Stoichiometric AFR and theoretical SB.

No	Biomass	Moisture	FC	VM	Ash	C	H	O	N	S	AFR	SB
1	Bagasse	50.00	12.23	83.01	4.76	46.74	6.03	42.25	0.13	0.08	5.26	0.67
2	Wheat	8.79	14.63	76.62	8.75	44.07	5.82	40.36	0.63	0.38	4.79	0.60
3	Cotton	7.92	18.46	77.81	3.73	45.46	5.89	43.80	0.67	0.45	5.08	0.66
4	Sesame	11.23	16.44	77.14	6.42	42.70	5.92	43.88	0.55	0.53	4.66	0.60
5	Groundnut	11.12	23.56	73.55	2.89	51.32	6.05	38.96	0.57	0.21	6.01	0.75
6	Sorghum	5.22	17.19	77.11	5.70	42.00	5.49	45.42	0.66	0.73	4.43	0.59
7	Millet	3.20	8.18	86.02	5.80	39.18	3.39	51.61	0.03	0.00	3.18	0.55
8	Banana	6.67	7.57	83.07	9.36	33.45	6.44	49.92	0.80	0.04	3.48	0.45
9	Sunflower	10.58	21.62	67.83	10.55	43.82	5.55	39.12	0.80	0.15	4.62	0.59
10	Maize	8.42	17.59	77.16	5.25	44.17	5.80	43.47	1.30	0.01	4.83	0.63

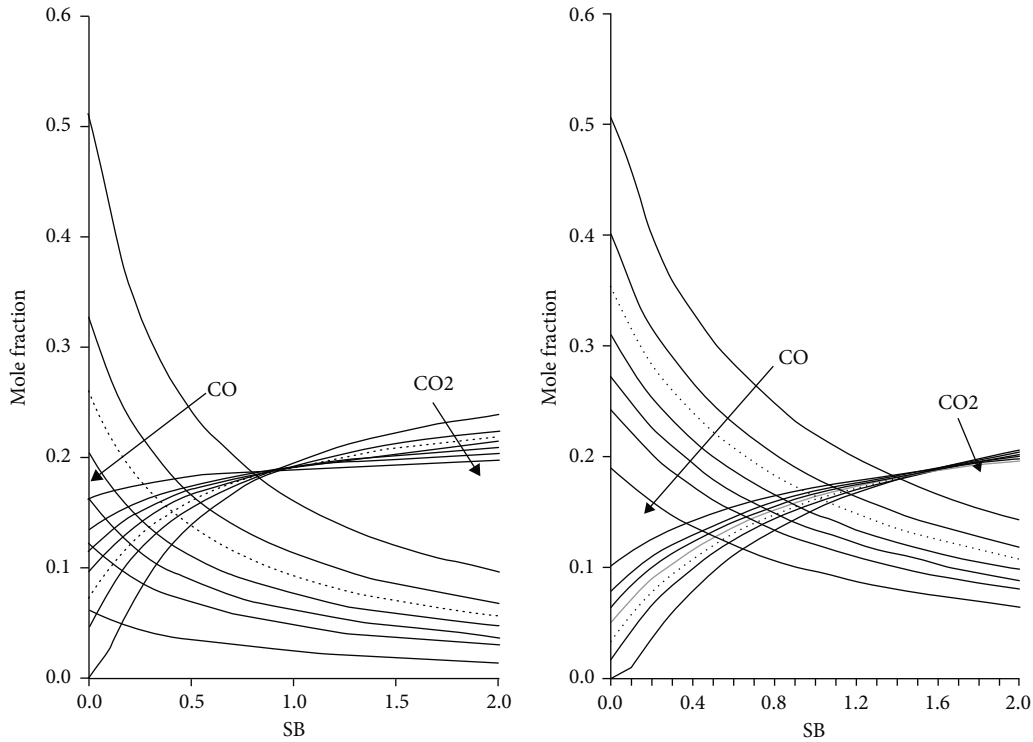

(a) Bagasse (b) Wheat

Figure 2: CO and CO_2 concentration vs. ER and SB. Dotted curves at ER = 0.15. The arrow indicates increasing ER.

crossover is located at a slightly higher SB than at CBP. This point may be coined as oxygen boundary point (OBP), where all oxygen (added and in the biomass) is depleted, the inception of water gas shift reaction. Explanation of this phenomenon may need further research.

3.3. Syngas Characteristics. Figures 6(a)–6(d) show syngas composition, LHV, H_2/CO ratio, and yield (syngas to biomass ratio). For all types of syngas, H_2 is 0.32-0.42 (mole fraction), CO is 0.13 to 0.16 (mole fraction), LHV is 5.0 and 8.0 MJ/kg, and the yield is ≥1.5. Wheat, groundnut, and sunflower have the best syngas characteristics while millet and bagasse have the poorest syngas characteristics. All biomasses except bagasse and millet have a carbon to nitrogen ratio (C/N) of 30 to 90 (Table 3) while the C/N ratios of bagasse and millet are 361 and 1387, respectively. Hence, C/N is a limiting factor. However, the author is unaware of such a finding and has no clear explanation of the correlation between C/N and syngas production.

Table 6 summarizes the gasification operation conditions (ER, SB, and T); syngas characteristics (composition, mole fraction, H_2/CO ratio, LHV, density, MW, and syngas to biomass ratio); and the potential production. The potential syngas production is 14.17 Mt/year (11 billion m^3/year).

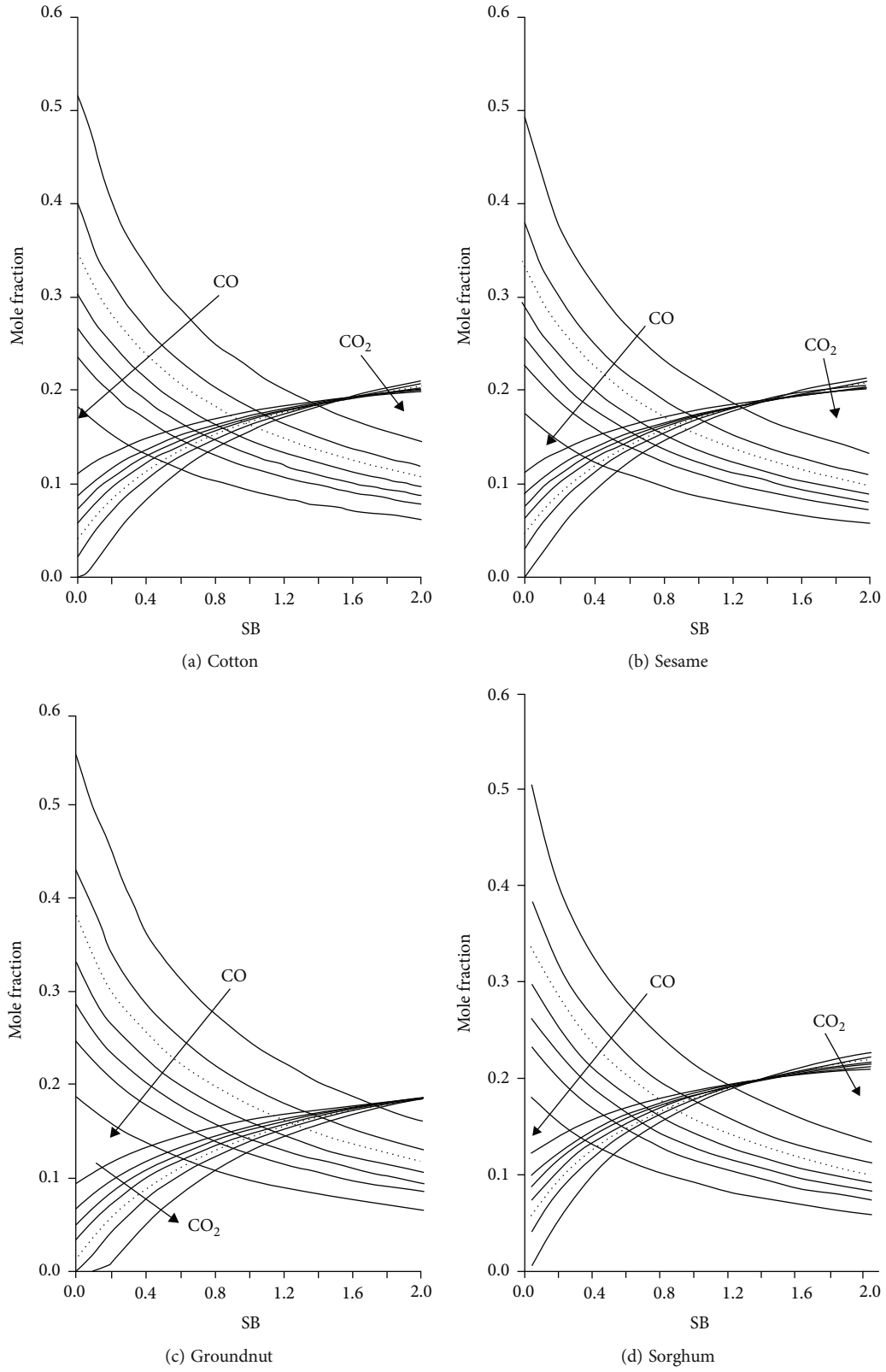

(a) Cotton (b) Sesame

(c) Groundnut (d) Sorghum

Figure 3: CO and CO_2 concentration vs. ER and SB. Dotted curves at ER = 0.15. The arrow indicates increasing ER.

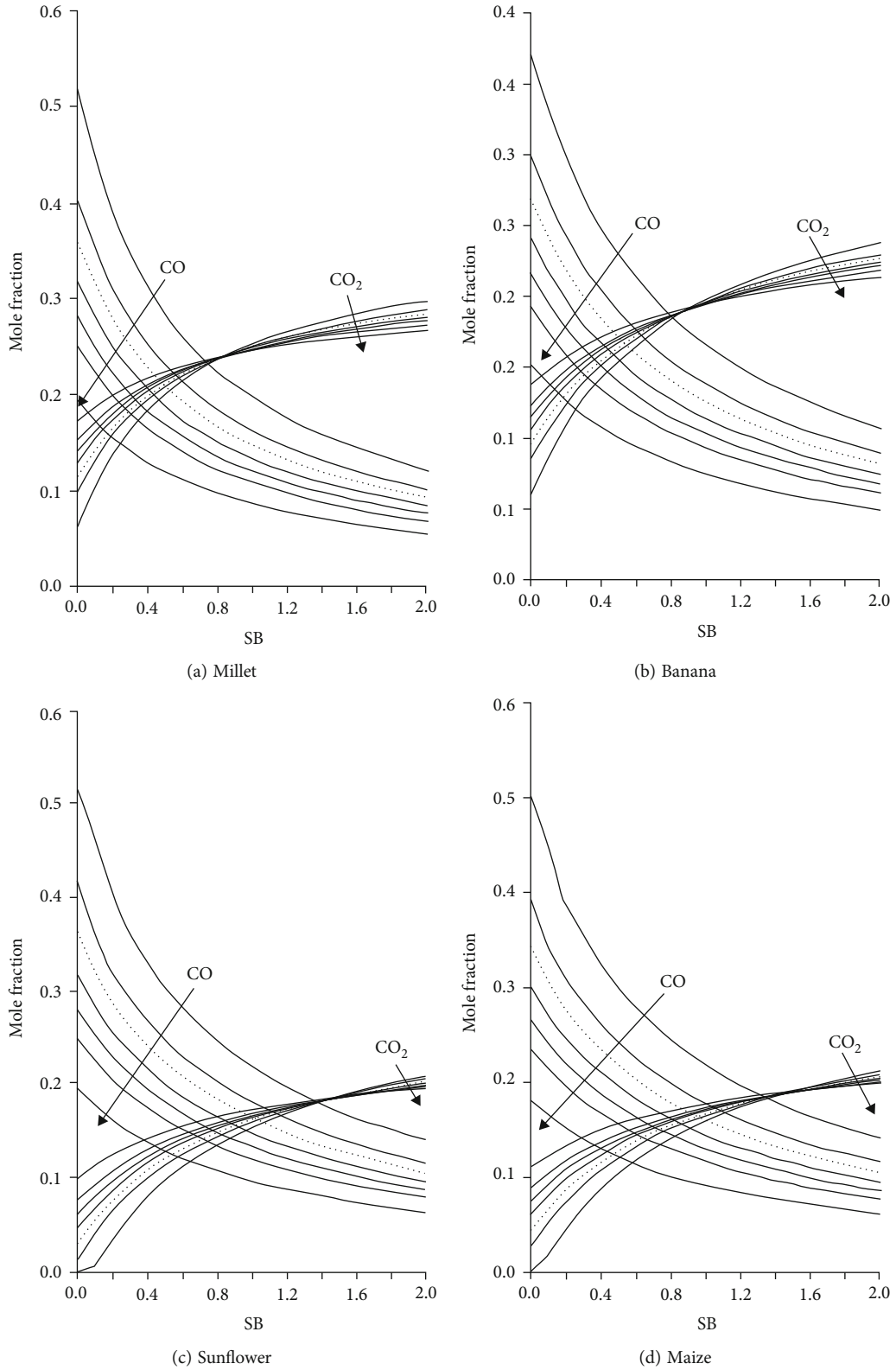

(a) Millet (b) Banana

(c) Sunflower (d) Maize

Figure 4: CO and CO_2 concentration vs. ER and SB. Dotted curves at ER = 0.15. The arrow indicates increasing ER.

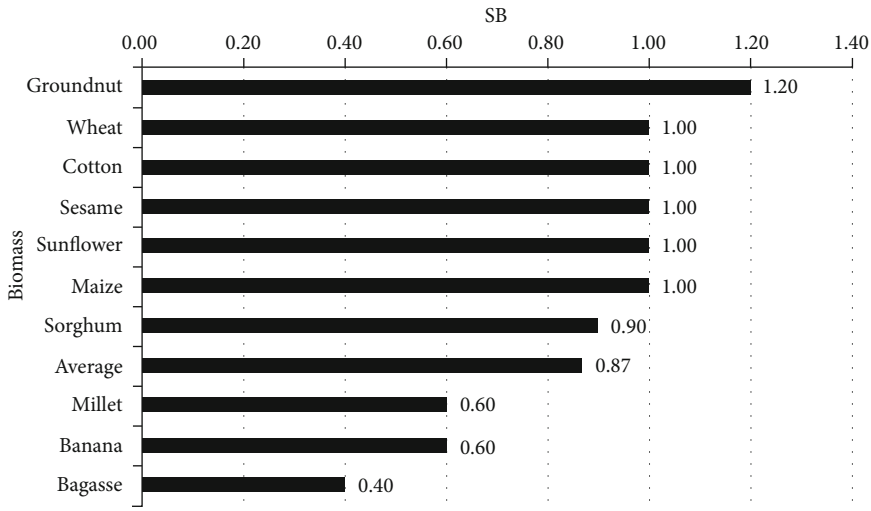

Figure 5: SB at ER = 0.15 for different types of biomass.

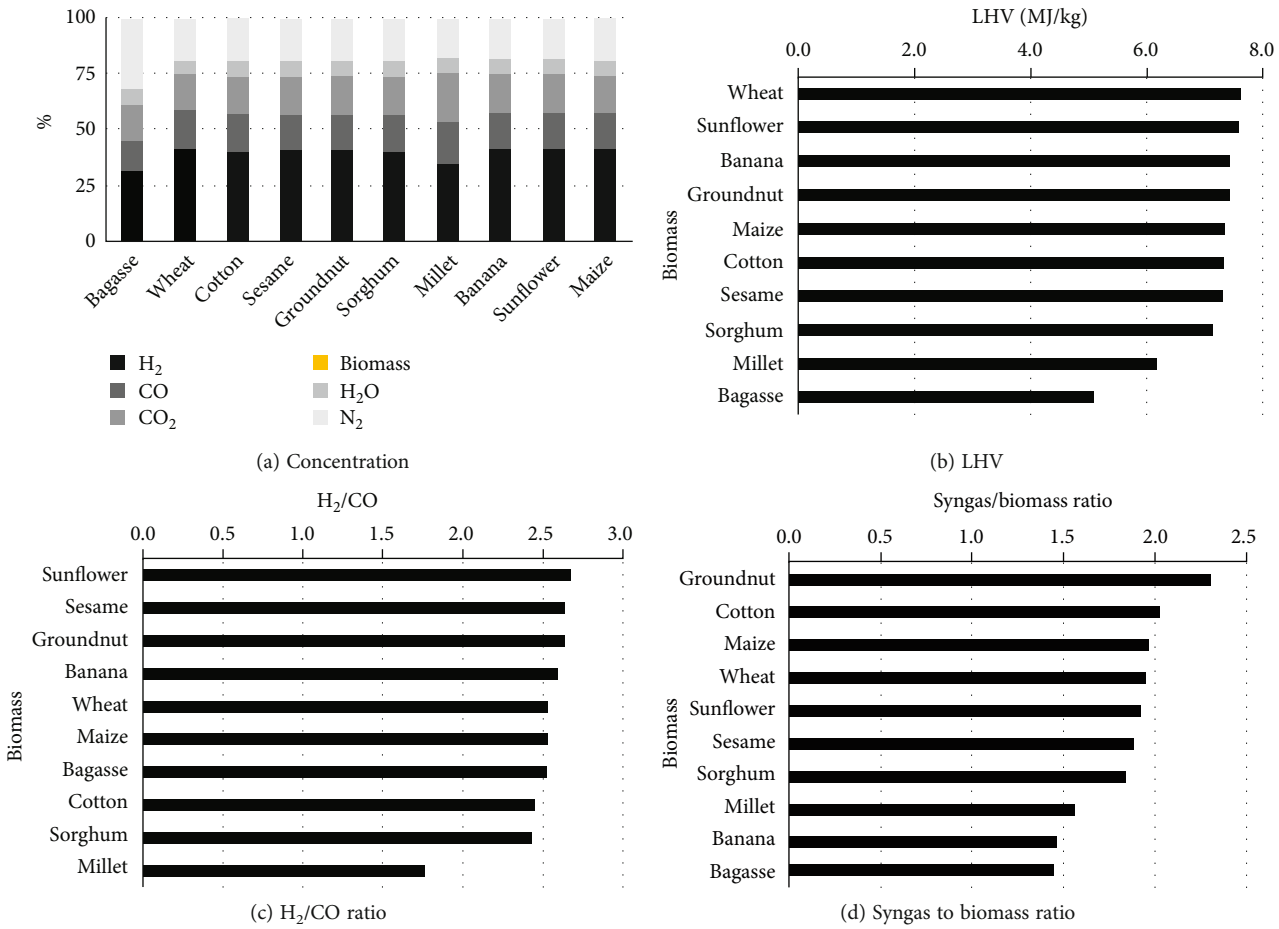

Figure 6: Syngas characteristics.

Table 6: Syngas characteristics at gasification temperature of 850°C.

Parameter	Bagasse	Wheat	Cotton	Sesame	Groundnut	Sorghum	Millet	Banana	Sunflower	Maize	Average
ER	0.15	0.15	0.15	0.15	0.15	0.15	0.15	0.15	0.15	0.15	0.15
SB	0.60	1.00	1.00	1.00	1.30	0.90	0.60	0.60	1.10	1.00	0.91
$\rho\ (\mathrm{kg/m^3})$	0.85	0.75	0.76	0.76	0.75	0.77	0.86	0.76	0.75	0.76	0.78
MW	21.88	19.19	19.58	19.50	19.29	19.88	22.07	19.42	19.17	19.51	19.95
M (kg/h)	14.46	19.46	20.23	18.83	23.04	18.43	15.67	14.65	19.22	19.60	18.36
LHV (MJ/kg)	5.10	7.63	7.32	7.31	7.43	7.14	6.18	7.44	7.60	7.36	7.05
Mole fraction											
H_2	0.32	0.42	0.40	0.41	0.41	0.40	0.34	0.41	0.42	0.41	0.39
CO	0.13	0.16	0.16	0.16	0.16	0.16	0.19	0.16	0.16	0.16	0.16
CO_2	0.17	0.16	0.17	0.17	0.16	0.18	0.22	0.17	0.17	0.17	0.17
CH_4	0.00	0.00	0.00	0.00	0.00	0.00	0.00	0.00	0.00	0.00	0.00
H_2O	0.06	0.06	0.06	0.06	0.06	0.06	0.06	0.06	0.06	0.06	0.06
N_2	0.33	0.20	0.20	0.20	0.21	0.20	0.18	0.19	0.19	0.20	0.21
Total	1.00	1.00	1.00	1.00	1.00	1.00	1.00	1.00	1.00	1.00	1.00
H_2/CO	2.52	2.53	2.46	2.64	2.64	2.43	1.76	2.59	2.68	2.52	2.48
Syngas/biomass	1.45	1.95	2.02	1.88	2.30	1.84	1.57	1.47	1.92	1.96	1.84
											Total
$\dot{M}_b$ (Mt/year)	0.66	0.06	0.01	0.15	0.35	4.85	1.52	0.38	0.04	0.02	8.04
$\dot{M}_S$ (Mt/year)	0.12	0.12	0.01	0.28	0.81	8.94	2.38	0.56	0.07	0.03	14.17
$\dot{V}_s\ (10^9\ \mathrm{m^3/year})$	0.09	0.09	0.01	0.21	0.61	6.92	2.05	0.42	0.06	0.02	11.00

These characteristics make syngas suitable for both energy and industry applications with exception of Millet which has $H_2/CO < 2$.

4. Conclusion

Biomass information on 10 agriculture residues is collected. The potential energy is estimated in Mtoe. A simulation program is tailored using Aspen plus software. The program is run for each type of biomass for a wide range of ER and SB. The data is analyzed, and the syngas characteristic for each syngas is established.

The work concluded that cotton stalks, sesame straw, groundnut shells, maize straw, sorghum straw, sunflower husks, wheat straw, and banana leaves produce syngas of high quality. Bagasse and millet straw produced syngas of poor quality. The work also concluded that the biomass gasification process is not fully understood. The work identified two points of equilibrium: the carbon boundary point (CBP) and the oxygen boundary point (OBP). However, OBP needs further investigation to be confirmed.

Data Availability

All information used to support the findings of the study is available from the corresponding author upon request.

Conflicts of Interest

The author declares that he has no conflicts of interest.

References

[1] A. A. Rabah, H. B. Nimer, K. R. Doud, and Q. A. Ahmed, "Modelling of Sudan's energy supply, transformation, and demand," *Journal of Energy*, vol. 2016, 14 pages, 2016.

[2] M. O. Abdeen, "Biomass energy potential and future prospect in Sudan," *Renewable and Sustainable Energy Reviews*, vol. 9, no. 1, pp. 1–27, 2005.

[3] M. Adams, "Technical report: forest products, harvesting and utilization component," *Paper Erciyes Tarımve Hayvan Bilimleri Dergisi ETHABD*, vol. 2, no. 2, pp. 35–38, 1995.

[4] B. Demirel, G. A. K. Gürdil, and O. Gadalla, "Biomass energy potential from agricultureal porduction in Sudan," *ETHABD*, vol. 2, no. 2, pp. 35–38, 2019.

[5] FAO, *National Investment*, Profile. Water for Agriculture and Energy, Sudan, 2015.

[6] M. O. Abdeen, "Focus on low carbon technologies: the positive solution," *Renewable and Sustainable Energy Reviews*, vol. 12, no. 9, pp. 2331–2357, 2008.

[7] C. Karaca, G. A. K. Gürdil, and H. H. Öztürk, "Determining and mapping agricultural¨ biomass energy potential in Samsun Province of Turkey," *ICOEST 3rd International Conference on Environmental Science and Technology*, vol. 1, pp. 34–43, 2017.

[8] A. Galvagnoa, M. Prestipinoa, V. Chiodob, S. Maisanob, S. Bruscaa, and R. Lanzafamec, "Energy performance of CHP system integrated with citrus peel air-steam gasification: a comparative study," *Energy Procedia*, vol. 126, no. 201709, pp. 485–492, 2017.

[9] M. Prestipino, F. Salmeri, F. Cucinotta, and A. Galvagno, "Thermodynamic and environmental sustainability analysis

of electricity production from an integrated cogeneration system based on residual biomass: a life cycle approach," *Applied Energy*, vol. 295, p. 117054, 2021.

[10] D. Cirillo, D. Cirillo, M. Di Palma et al., "A novel biomass gasification micro-cogeneration plant: experimental and numerical analysis," *Energy Conversion and Management*, vol. 243, article 114349, 2021.

[11] A. M. Abdalla, T. H. Hassan, and M. E. Mansour, "Performance of wet and dry bagasse combustion in Assalaya Sugar Factory-Sudan," *Innovative Energy & Research*, vol. 7, p. 1, 2018.

[12] S. Begum, M. G. Rasul, D. Akbar, and N. Ramzan, "Performance analysis of an integrated fixed bed gasifier model for different biomass feedstocks," *Energies*, vol. 6, no. 12, pp. 6508–6524, 2013.

[13] F. Tan, L. He, Q. Zhu, Y. Wang, G. Hu, and M. He, "Characterization of different types of agricultural biomass and assessment of their potential for energy production in China," *BioResources*, vol. 14, no. 3, pp. 6447–6464, 2019.

[14] S. B. Jamaldheen, P. B. Saynik, V. S. Moholkar, and A. Goyal, "Fermentation and pyrolysis of finger millet straw: significance of hydrolysate composition for ethanol production and characterization of bio-oil," *Bioresource Technology Reports*, vol. 13, p. 100630, 2021.

[15] P. Basu, *Combustion and Gasification in Fluidized Beds*, vol. 1, RC Press, California, 2006.

[16] W. Jangsawang, K. Laohalidanond, and S. Kerdsuwana, "Optimum equivalence ratio of biomass gasification process based on thermodynamic equilibrium model," *Energy Procedia*, vol. 79, pp. 520–527, 2015.

[17] W. Jangsawang, A. Klimanek, and A. K. Gupta, "Enhanced yield of hydrogen from wastes using high temperature steam gasification," *Journal of Energy Resources Technology, Transactions of the ASME*, vol. 128, no. 3, pp. 179–185, 2006.

[18] R. N. Kumara and V. Aarthib, "From Biomass to Syngas, Fuels and Chemicals – A Review," *AIP Conference Proceedings*, vol. 2225, pp. 1–4, 2020.

[19] A. K. Varmaa, L. S. Thakur, R. Shankar, and P. Mondala, "Pyrolysis of wood sawdust: effects of process parameters on products yield and characterization of products," *Waste Management*, vol. 89, no. 89, pp. 224–235, 2019.

[20] A. Mavukwana, K. Jalama, F. Ntuli, and K. Harding, "Simulation of sugarcane bagasse gasification using Aspen Plus," *International Conference on Chemical and Environmental Engineering (ICCEE'2013)*, 2013, Johannesburg, South Africa, April 2013, 2013.

[21] A. Gonzalez-Diaz, J. C. Sánchez Ladrón de Guevara, L. Jiang, M. O. Gonzalez-Diaz, P. Díaz-Herrera, and C. Font-Palma, "Techno-environmental analysis of the use of green hydrogen for cogeneration from the gasification of wood and fuel cell," *Sustainability*, vol. 13, no. 6, p. 3232, 2021.

[22] M. A. Elbager, X. L. Edreis, C. Xu, and H. Yao, "Kinetic study and synergistic interactions on catalytic CO_2 gasification of Sudanese lower sulphur petroleum coke and sugar cane bagasse," *Journal of Materials Research and Technology*, vol. 6, no. 2, pp. 147–157, 2017.

[23] B. S. Subbaiah, D. K. Murugan, D. B. Deenadayalan, and M. I. Dhamodharan, "Gasification of biomass using fluidized bed," *International Journal of Innovative Research in Science, Engineering and Technology*, vol. 3, no. 2, pp. 8995–9002, 2014.

[24] D. Chen, E. Shuang, and L. Liu, "Analysis of pyrolysis characteristics and kinetics of sweet sorghum bagasse and cotton stalk," *Journal of Thermal Analysis and Calorimetry*, vol. 131, no. 2, pp. 1899–1909, 2018.

[25] I. Kabenge, G. Omulo, N. Banadda, J. Seay, A. Zziwa, and N. Kiggundu, "Characterization of banana peels wastes as potential slow pyrolysis feedstock," *Journal of Sustainable Development.*, vol. 11, no. 2, pp. 14–9063, 2018.

[26] T. Zheliezna, B. Wern, and B. Peregudov, "Report No. 3: Estimation of biomass potential in Odesa oblast. Selection of biomass feedstock and technologies for energy production in conditions of Kylyysky and Shyryayvsky rayons," in *Recommendations for the implementation of the most effective types of bioenergy projects*, Biomass-Carbon LTD and GIZ, 2017.

[27] S. Garivait, U. Chaiyo, S. Patumsawad, and J. Deakhuntod, "Physical and Chemical Properties of Thai Biomass Fuels from Agricultural Residues," in *The 2nd Joint International Conference on Sustainable Energy and Environment*, Bangkok, Thailand, November 2006.

[28] A. F. Pérez, J. L. Llanes, and M. G. Cortés, "Bagasse gasification to increase electricity generation in Cuban sugar mills," *Proceedings of the International Society of Sugar Cane Technologists*, vol. 30, pp. 1673–1681, 2019.

[29] P. De Filippis, C. Borgianni, M. Paolucci, and F. Pochetti, "Gasification process of Cuban bagasse in a two-stage reactor," *Biomass and Bioenergy*, vol. 27, no. 3, pp. 247–252, 2004.

[30] W. Doherty, A. Reynolds, and D. Kennedy, "The effect of air preheating in a biomass CFB gasifier using ASPEN Plus simulation," *Biomass and Bioenergy*, vol. 33, no. 9, pp. 1158–1167, 2009.

[31] F. Paviet, F. Chazarenc, and M. Tazerout, "Thermo chemical equilibrium modelling of a biomass gasifying process using ASPEN PLUS," *International Journal of Chemical Reactor Engineering*, vol. 7, no. 1, pp. 1–16, 2009.